Supporting Information for

Rapid identification of P-C bond in phosphorus-carbon anode materials

Yadong Ye, Qiang Xiao, Huanyu Xie, Hongchang Jin*, Hengxing Ji*

*Corresponding author: jhckimi@ustc.edu.cn; jihengx@ustc.edu.cn

This file includes:

Synthesis of phosphorus-carbon composites

The black phosphorus and graphite were well mixed with a mass ratio of 1:1 and sealed in the jar at an argon-filled glove box with stainless steel balls. The ball mill jar was performed with a rotation rate of 30 HZ for 20h by HEBM (high energy ball milling). The black phosphorus-carbon composite (BP-G) can be obtained. Synthesis of the mixture of black phosphorus and graphite (BP/G): The ball-milled black phosphorus and ball-milled graphite were mixed by mechanical stirring in glove box to obtain the BP/G. The red phosphorus-carbon composites (RP-G) and the mixture of red phosphorus and graphite (RP/G) were synthesized in the same way of black phosphorus.

During the synthesis of BP-G and RP-G, although the milling jar was filled with argon for protection, its gas-tightness is limited, and prolonged high-energy milling can lead to slight oxidation of the surfaces of BP-G and RP-G. Consequently, P-O bond signals can be observed in BP-G and RP-G (Figures 4a, b). In contrast, BP/G and RP/G were produced by a secondary mechanical grinding and mixing of the milled phosphorus and graphite under argon protection within the glove box. Due to this argon atmosphere, the secondary grinding not only prevents further oxidation of the samples but also disrupts the surfaces of the original particles, exposing fresh, unoxidized areas. As a result, no P-O bond signals are detected in BP/G and RP/G (Figures 4c, d).

Electrochemical Measurements

The active material, Ketjenblack, and poly (vinylidene difluoride) (PVDF) were mixed in a mass ratio of 8:1:1, and appropriate amount of N-methyl pyrrolidone (NMP) was added and stirred and mixed to form a slurry, which was coated on a copper foil (12 μm thick), and then dried under vacuum at 60°C for 24 hours to obtain the electrode sheets. The mass loading of the electrodes was about 2.2 mg/cm^2 and the areal capacity of the electrodes was about 1.8 mAh/cm^2, where the capacity was calculated based on the total mass of the composite. The half-cell consists of a phosphorus composite cathode, a lithium metal anode, a polypropylene (pp) separator, and an electrolyte containing 1 M LiPF6 in ethylene carbonate/diethylene carbonate (EC/DEC) with 5% fluoroethylene carbonate (FEC). The charge/discharge tests were performed using the

LAND and NEWARE battery test system with a voltage window of 0.01-2.0V.

Structural Characterizations

Raman spectra was performed on a Renishaw in via Raman spectrometer with a 532 nm incident laser excitation (laser spot size of 0.5 μm). FT-IR spectra was obtained using a Nicolet 8700 Infrared spectrometer with KBr powder as carrier. The C K-edge XAS spectra were measured on beamline BL12B of the National Synchrotron Radiation Laboratory, Hefei, using the total electron yield mode. XPS spectra were performed on an ESCA Lab MKII with an excitation source of Mg Kα radiation (1253.6 eV). Solid state NMR experiments are performed in a 9.5 T magnetic field with a Bruker 400 MHz AVANCE III spectrometer. In an argon-filled glove box, the active material was loaded into a 1.3 mm rotor. Solid State ^{31}P Magic-Angle Spinning (MAS) NMR spectra were obtained using Hahn-echo pulses (90° pulse-τ to 180° pulse-τ) at a spinning frequency of 55 kHz. In order to obtain quantitative ^{31}P NMR spectra, a cyclic delay of 120 s is used for the full relaxation of excited magnetization. The chemical shifts of the ^{31}P reference adenosine diphosphate (1 ppm).

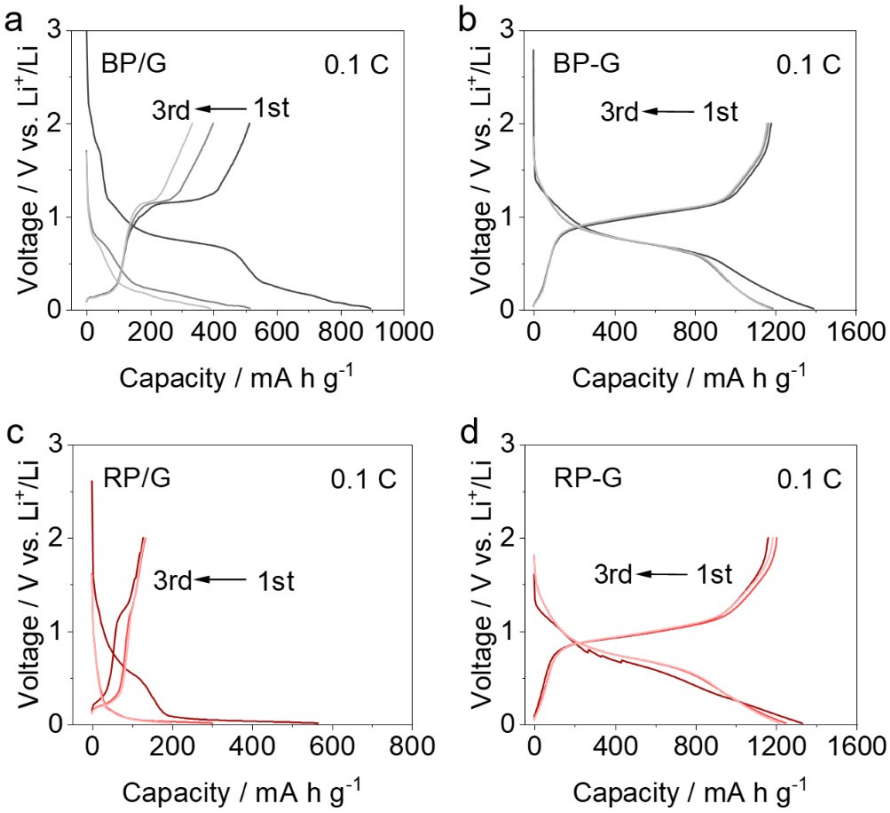

Figure S1. The discharge-charge profiles of BP/G(a), BP-G(b), RP/G(c), and RP-G(d). Considering the theoretical capacity of the phosphorus-carbon composite as 1300 mA h/g, the corresponding 1C current is 1.3 A/g and 0.1C current is 0.13 A/g.

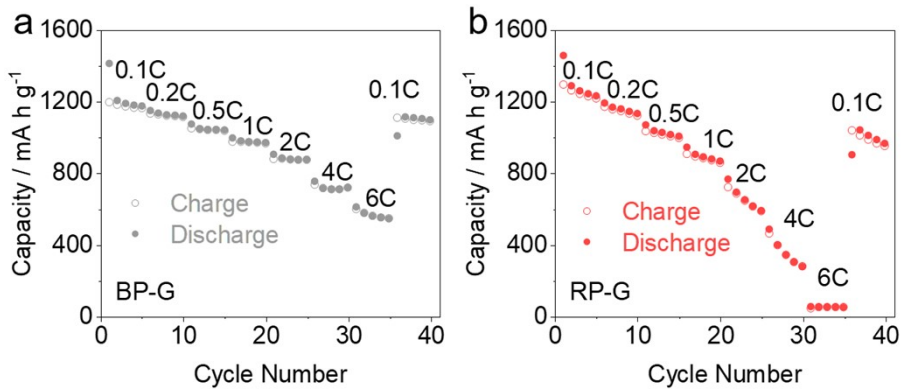

Figure S2. The C-rate capability of BP-G(a), and RP-G(b).

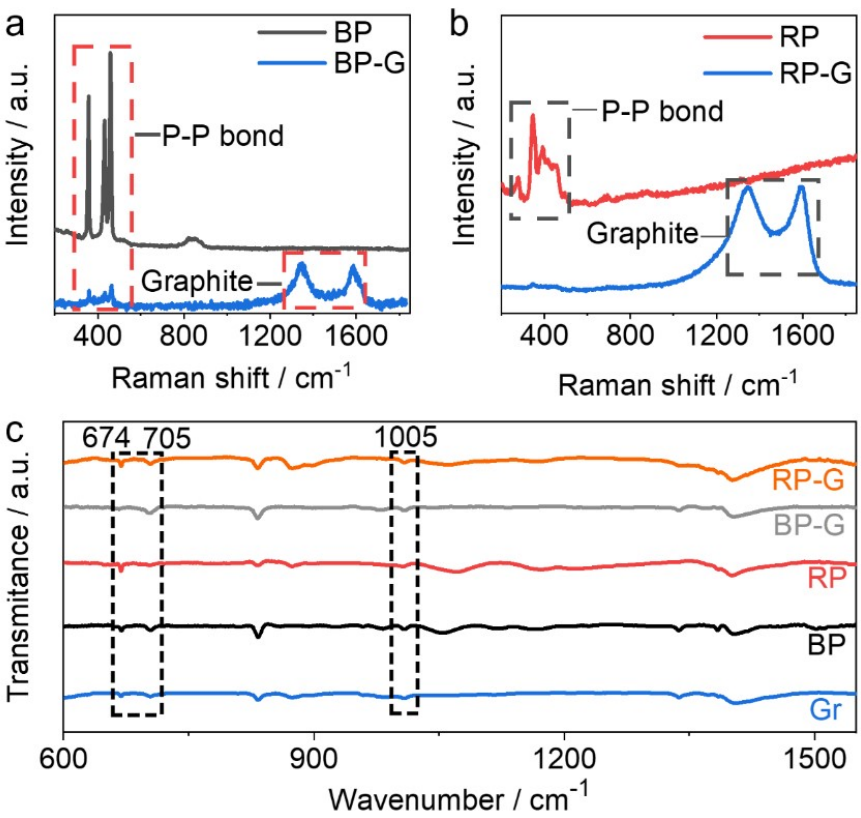

Figure S3. Raman spectrum of BP and BP-G(a), RP and RP-G(b). (c)Comparisons of FT-IR spectra between the Gr, BP, RP, BP-G, RP-G.

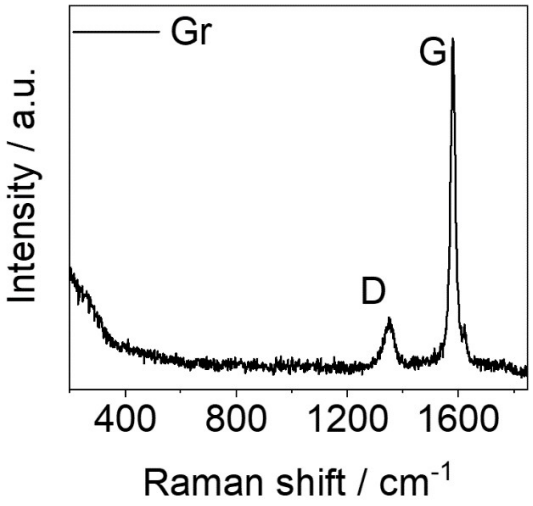

Figure S4. The Raman spectrum of pure graphite.

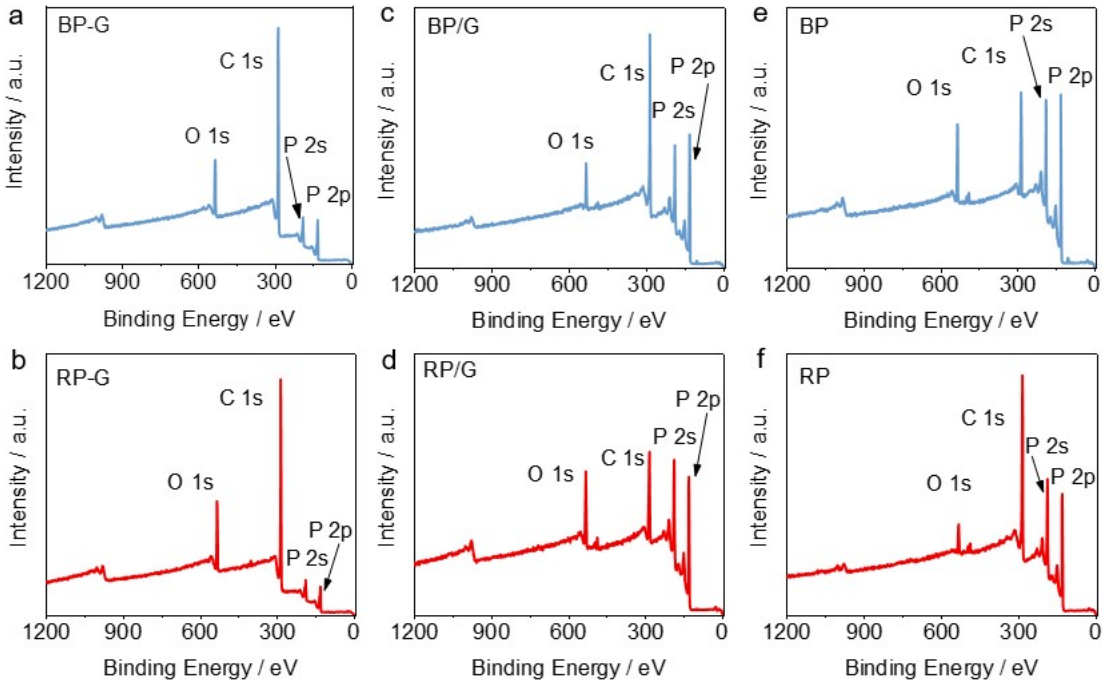

Figure S5. The XPS general spectrum of BP-G(a), RP-G(b), and BP/G(c), RP/G(d), BP(e), RP(f).

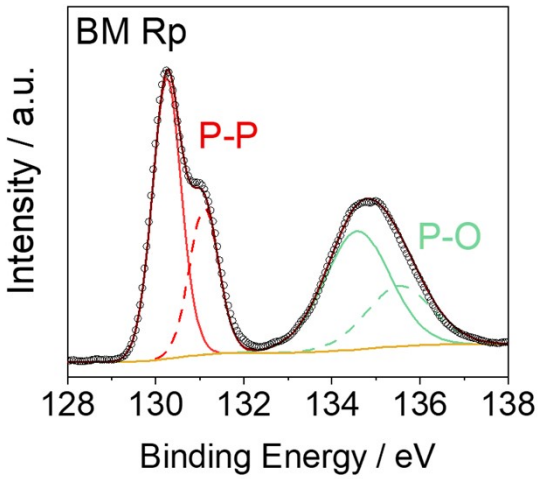

Figure S6. The X-ray photoelectron P2p-spectra of RP powder obtained by high energy ball milling.

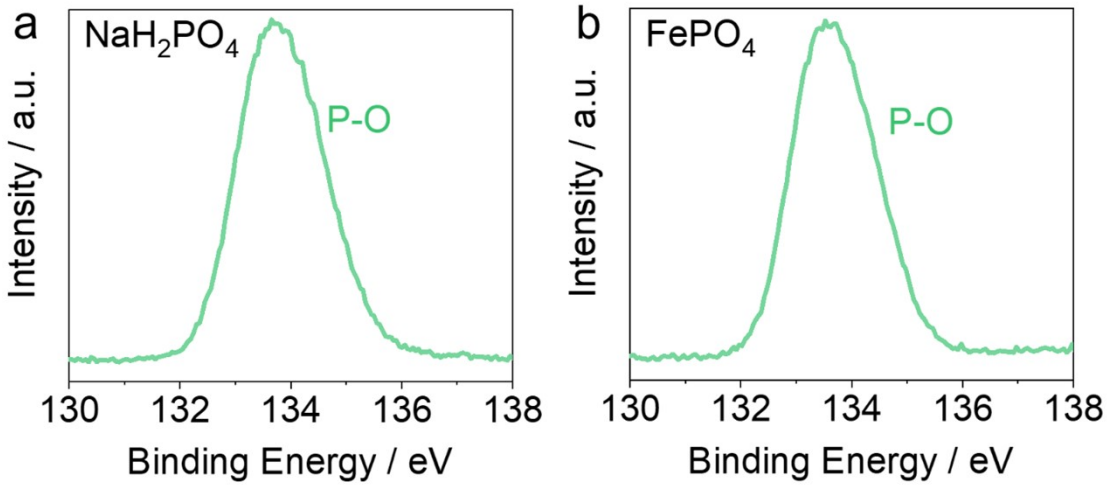

Figure S7. The X-ray photoelectron P2p-spectra of NaH_2PO_4 (a) and $FePO_4$ (b).

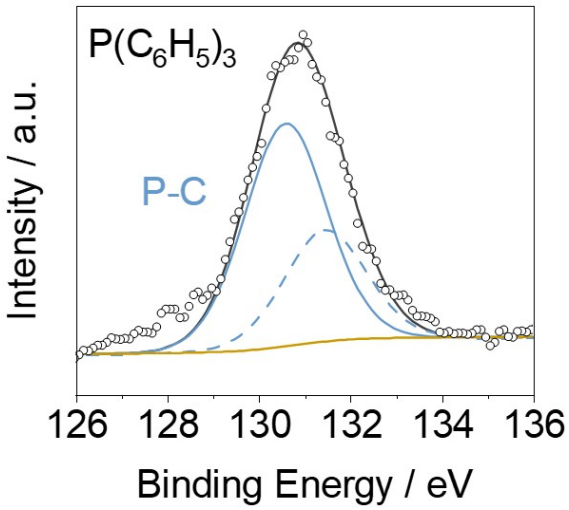

Figure S8. The X-ray photoelectron P 2p-spectra of triphenylphosphine.